XLI CILAMCE
XLI Ibero-Latin American Congress on Computational Methods in Engineering
16-19 November, 2020 FOZ DO IGUAÇU PARANÁ - BRAZIL

Numerical simulation of the effect of zinc chloride flux on ATIG welding of aluminum

Larissa Mikaele Ribeiro Adriano[1], Paulo Justiniano de Oliveira Junior[1], Cláudio Parreira Lopes[1], Wagner Custódio de Oliveira [1]

[1]*Dept. of Mechatronics Engineering, Centro Federal de Educação Tecnológica de Minas Gerais,*

Álvares de Azevedo St, 400, Divinópolis, Minas Gerais, Brazil.

larissa.adriano97@gmail.com, paulojus444@hotmail.com, claudio@cefetmg.br, wagnercoliveira@cefetmg.br

Abstract. In this work, a study based on numerical simulation methods was applied to Activated Tungsten Inert Gas welding (ATIG welding), a simple variant of TIG welding that consists only of applying a thin layer of flux immediately before welding. A Finite Element Analysis (FEA) method was used to compare the aluminum TIG and ATIG weld pool to evaluate the effect of zinc chloride flux on the geometric parameters of the ATIG weld bead. Previous tests have shown that this flux allows an improvement in the final appearance of the weld surface, possibly due to the removal of the alumina layer, in addition to a small gain in the penetration of the weld bead using negative direct current instead of positive direct current and alternating currents, commonly used for welding aluminum. The results have shown that a possible removal of the alumina layer by the zinc chloride flux on the aluminum ATIG welding does not influence the weld bead geometry. This result is similar to the outcomes of other experimental works in the literature.

Keywords: simulation, ATIG welding, zinc chloride.

1 Introduction

Aluminum and its alloys continue to grow in acceptance, particularly in the automotive industry. The electronics industry is another major user of cast aluminum for chassis, enclosures, terminals and others. Aluminum alloy castings are produced by virtually all commercial processes in a range of compositions possessing a wide variety of useful engineering properties [1]. Therefore, studies for the development or optimization of joining processes for welding aluminum and its alloys, with quality and low cost, have been of fundamental importance.

The TIG welding process (or GTAW, Gas Tungsten Arc Welding) is used when good weld appearance and high quality of welding is required. In this process, an electric arc is formed between a tungsten electrode and the base metal. The arc region is protected by an inert gas or mixture of gases. The tungsten electrode is heated to temperatures high enough for the emission of the necessary electrons for the operation of the arc [2].

Activating welding (ATIG) is a welding process with high efficiency of production, high quality, low energy consumption and low cost. In activated TIG welding, a thin layer of halides, oxides, or sulfides is applied to the surface to remove the metal oxide layer of the welded joint or to obtain a gain of penetration for some materials. In order to produce this activated flux paste, the base flux material is mixed appropriately with either acetone or ethanol in a ratio of 1:6 [3]. Then, the activated flux is deposited over the work-piece with the use of a brush. Other approaches of flux deposition are made of flux and solvent mixture with the help of aerosol applicators to ensure uniform flux coating [4]. This new welding process has been successfully applied in the field of TIG welding and generates a new welding process called “active flux TIG welding”, namely ATIG welding [5]. However, there are not commonly agreed mechanisms for the increase in penetration depth yet, despite the several ones proposed in the literature [6]. Some researchers [7] believed that the arc constriction increased the current density at the anode root and then a substantial increase in penetration depth could be achieved. It has been

considered that the arc constriction is produced by the effect of vaporized flux molecules, namely oxygen or halogens, capturing electrons in the outer (cooler) regions of the arc, due to their higher electron affinity.

Heiple and Roper [8] proposed that the changes in the magnitude and direction of surface tension gradients on the weld pool surface caused by surface active elements such as oxygen and sulphur could change the direction of fluid flow (Marangoni convection) on the ATIG weld pool.

Thus, a numerical simulation of effects of activating flux on flow patterns and weld penetration on ATIG welding has been developed, using a mathematical model to describe a molten pool of three-dimensional gas tungsten arc welding due to a moving arc. It considered the surface tension temperature gradient as a function of temperature and oxygen concentration to simulate the effect of activating flux on flow patterns and weld penetration [9]. The authors have concluded that the change in the surface tension gradient in the molten pool is considered to be the main mechanism for increased penetration in ATIG welding. Arc constriction and voltage increase can cause deeper penetration and narrow the width of the weld. However, this is still not the main mechanism for increased penetration.

A previous work [10] has shown that zinc chloride flux allows an improvement in the final appearance of the weld surface. Possibly it happens due to the removal of the alumina layer, in addition to a small gain in the penetration of the ATIG weld bead using negative direct current, replacing positive direct current and alternating current, which are commonly used for aluminum welding.

The study used a Finite Element Analysis (FEA) method to compare the aluminum TIG and ATIG weld pool, evaluating thus the effect of zinc chloride flux on the geometric parameters of the ATIG weld bead.

2 Finite Element Analysis

2.1 Simulation Conditions

The simulation of the TIG welding process was carried out on an upper joint of an ASTM 1200-H14 aluminum plate, 150.0 mm long, 50.0 mm wide and 6.35 mm thick. In order to simulate the effect of zinc chloride on ATIG welding, considering that alumina was removed by the flux, an alumina layer was initially considered on TIG welding condition in half of the sample. The other half of the sample, on the other hand, did not have this layer for the ATIG welding (Figure 1). To effectively analyze the influence of the alumina layer on geometric parameters weld beads, the values of 0.03 mm, 0.06 mm, 0.09 mm, 0.12 mm and 0.15 mm were simulated as its possible thicknesses.

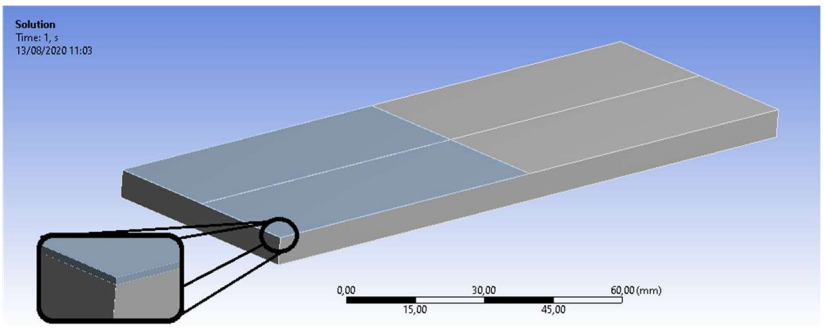

Figure 1. Aluminum plate displaying the thickness in detail of the alumina layer considered on TIG welding

The aluminum plate was three-dimensionally simulated in the Ansys software. The simulated welding parameters are given in Table 1.

Table 1. Simulated welding parameters

Parameters	Value
Welding Speed (mm/s)	3.33
Welding current (A)	120
Arc Voltage (V)	18

Arc efficiency (η)	0.65
Radius of the Beam (mm)	1.6

Welding speed and current, beam radius and welding voltage were based on the experiments carried out by Barroso et.al [10]. The arc efficiency was based on studies by Marques & Modenesi [11], in which it seems that for TIG welding in direct current with negative electrodes the efficiency values can vary from 0.5 to 0.80. Thus, the chosen value is the average between these two.

In order to produce well-graded finite element meshes, the geometric model was partitioned into several regions. Mesh quality is a feature of great importance in obtaining satisfactory results using the finite element method. Better results are achieved with homogeneous meshes and closer to the structured ones, containing a greater quantity of high-quality elements. The quality of the elements is defined based on the comparison to the ideal element, i.e. the base element in the formulation of the numerical method. In quadrilateral meshes, similar to a square, the criterion for comparing elements identifies the difference between the sides of the element and its internal angles. [12]

Considering that the specimen used was rectangular, a regular/structured mesh was sought, with topologically standardized nodes. To create the same in both working bodies, of different thicknesses, the body sizing method was used, in which it is possible to define the size of elements in a localized way, allowing to define the size in millimeters or to choose the number of divisions in a given edge. Each element was partitioned in 1.5 mm, providing a homogeneous mesh for analysis purposes. The number of nodes in the generated grid was 92812, still having 18700 elements. The thermo-physical properties of aluminum and aluminum oxide considered are shown in Table 2.

Table 2. Materials properties for aluminum and alumina.

Property	Aluminum	Alumina
	Value	
Density (kg/m³)	2719	3960
Specific Heat (J/KgºC)	871	850
Isotropic thermal conductivity(W/mºC)	202,4	35
Melting point (ºC)	660	2072

Source: Ansys materials library

For this simulation, three methods of heat transfer were considered: conduction, which can be described as a heat transfer mechanism between solids or fluids at rest; convection, when there is movement of the fluid, naturally or caused by an external force [13]; and radiation, when a particular body is heated up and starts to emit electromagnetic radiation, thus the spectrum of its radiation is directly linked to the temperature of the body, dependent in some way on its chemical composition [14].

2.2 Heat source model

Modeling the Gaussian heat source in motion can be used to simulate welding or laser cutting processes, predicting how much heat is needed to place in an object, as well as the speed at which it dissipates. Using the moving heat source plugin, it is possible to use the model for a moving heat source, inserting only the necessary inputs, such as the face of the body to which the heat flow in motion will be applied, the path of the heat source, the speed, the radius and the energy intensity of the heat source.

The faces used were the upper faces of the specimen. Bearing in mind that the specimen is 150 mm long and the weld path extends throughout this length, traced exactly in the center of the specimen, the value chosen for discretizing the heat source was 1000 welding steps.

As shown in the studies by Cangâni (2010) [14], fusion welding is carried out by applying concentrated energy to a part of the piece where the weld will be carried out, in order to achieve its localized fusion, preferably thermally affecting the rest of the piece minimally. For the sake of effectiveness in fusion welding, the electrical source must supply energy at a sufficiently high rate in an area small enough A_0 $[m^2]$ to guarantee localized fusion of the metal before the heat is diffused in quantities appreciable for the rest of the piece [11]. To characterize this process, the specific power of an energy source is defined as shown in equation (1),

$$Q"_{esp} = \eta \cdot \frac{E}{t \cdot A_0} \tag{1}$$

in which E represents the amount of energy generated by the heat source [J], η is the thermal yield and represents the fraction of energy effectively transferred by the torch to the specimen, t is the operating time given in [s], A_0 refers to the area defined by the weld bead and $Q"_{esp}$ is given in [W/m²].

For the electric arc, the energy generated per unit of time can be replaced by the product of voltage V by current I, reaching equation (2) for specific power.

$$Q"_{esp} = \frac{VI \cdot \eta}{A_0} \tag{2}$$

Rearranging equation (2) it is possible to define the thermal yield of the TIG welding process, as presented in (3).

$$\eta = \frac{Q"_{esp}}{Q"_{exp}} \cdot 100 \tag{3}$$

Knowing $Q"_{exp}$ is the power supplied by the welding torch, this can be represented by the equation (4).

$$Q"_{exp} = \frac{VI}{A_0} \tag{4}$$

Therefore, it is clear that the intensity of the heat source used can be obtained using (5).

$$Q"_{esp} = \eta \cdot \frac{VI}{A_0} \tag{5}$$

The value obtained through the previous mathematical formulations was 174.62 W / mm². It is important to note that the heat source for the TIG and ATIG process is the same, with the processes being differentiated only by activating the flow, in which the main hypothesis is to remove the alumina layer. For this process, the complete removal of the alumina layer was considered to evaluate the effect of zinc chloride flux on the geometric parameters of the aluminum ATIG weld bead.

Results and Discussions

Figures 2 and 3, respectively, show the temperature distribution when the torch passes along the entire direction of the specimen length with an alumina layer of 0.03 mm and 0.15mm on the TIG portion of the weld, and on ATIG portion, without oxide layers.

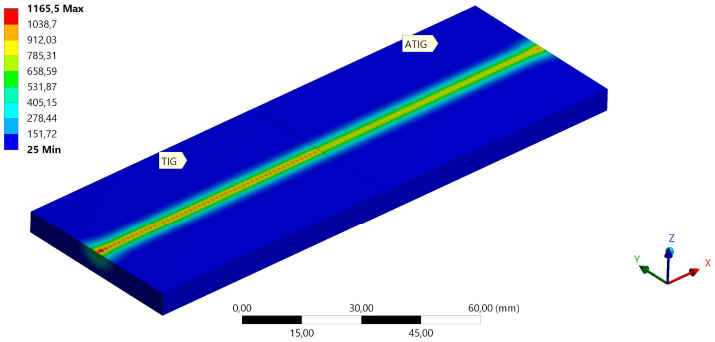

Figure 2. Three-dimensional temperature distribution with 0.03mm alumina layer.

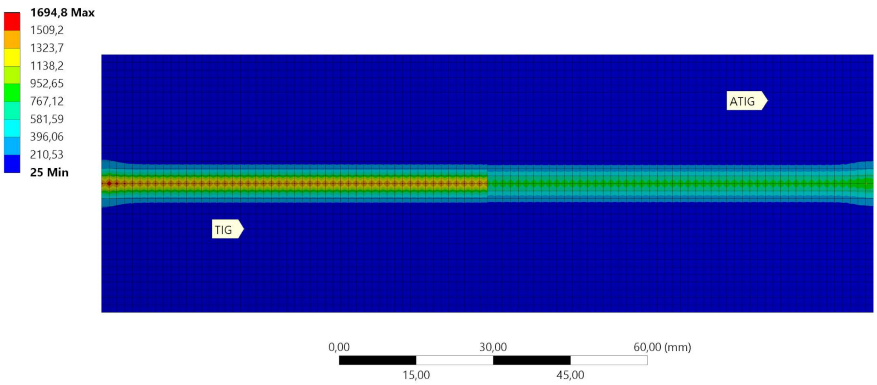

Figure 3. Temperature distribution with 0.15mm alumina layer.

In the TIG weld portion the aluminum oxide layer, due to its poor thermal conductivity, achieves higher temperatures: up to 1694.8ºC with a 0.15mm layer and 1165.5ºC when a 0.03mm alumina layer is considered. This maximum temperature difference also comes from the thermal conductivity factor, since with a thicker oxide layer the heat flow to the aluminum will be reduced and the oxide temperatures will be higher.

Figure 4 shows the cross section of the sample with all the different thicknesses of the alumina layers used. These sections were used to analyze the weld pool geometry characteristics. There is no visual change on the weld pool geometry, but using software tools it is possible to confirm that the TIG weld pool volume, when the alumina layer of 0.03mm is considered, is 14.2% minor than the TIG weld pool volume with 0.15mm.

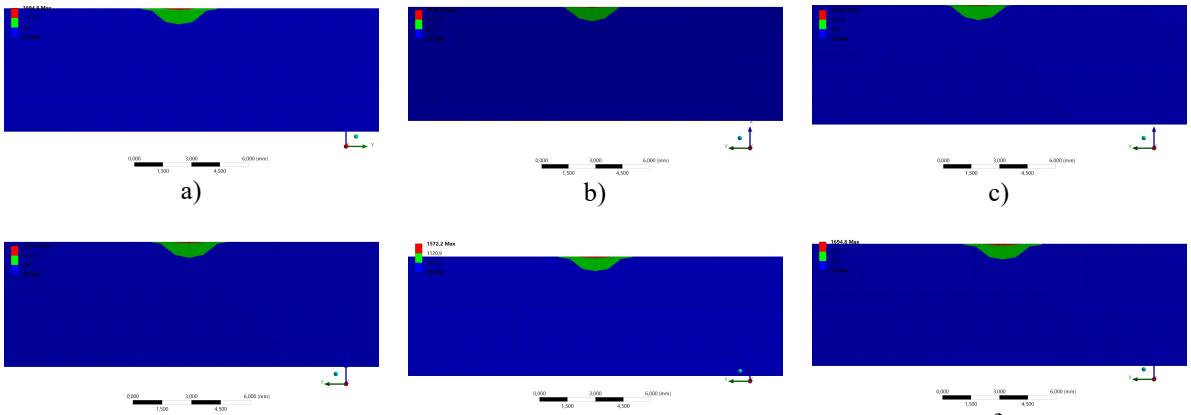

Figure 4. Weld pool cross section: a) 0.00mm oxide layer (ATIG); b) 0.03mm oxide layer; c) 0.06mm oxide layer; d) 0.09mm oxide layer; e) 0.12mm oxide layer; f) 0.15mm oxide layer

Table 3 shows the values of depth, width and area of aluminum weld beads.

Table 3. Weld pool dimensions according to Aluminum oxide layer thickness

Aluminum oxide layer (mm)	Depth (mm)	Width(mm)	Area(mm²)
0.00(ATIG)	0.682 ± 0.006	2.780± 0.006	1.253± 0.0014
0.03	0.757± 0.006	2.987± 0.006	1.455± 0.0014
0.06	0.713± 0.006	2.845± 0.006	1.409± 0.0014
0.09	0.699± 0.006	2.803± 0.006	1.377± 0.0014
0.12	0.664± 0.006	2.781± 0.006	1.283± 0.0014
0.15	0.647± 0.006	2.685± 0.006	1.248± 0.0014

It is possible to check a maximum difference of 0.207mm on width and 0.093mm on depth of the weld bead. Considering that the real alumina layer thickness has 3nm, we concluded that changing the thickness of the alumina layer from 0 to 0.15mm has little influence on the geometry parameters of TIG and ATIG weld beads. In this study, with oversized layers of alumina, the impact on the weld bead geometry was not as relevant as expected because the alumina layer prevents the passage of electric current hindering the TIG welding with negative direct

current. With an increase in the thickness of the alumina layer by 400%, the reduction in the volume of the weld bead was of only 14.22%.

Figure 5 shows the relation between alumina layer and Depth / Width (D/W) ratio.

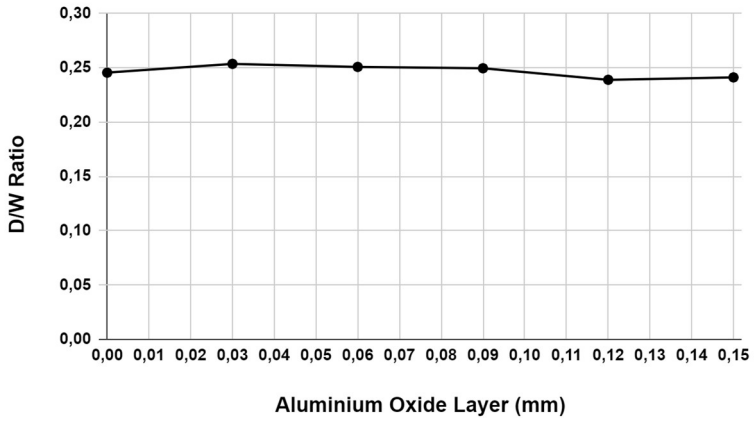

Figure 5. Relation between alumina layer thickness and D/W ratio.

The analysis of this figure shows that a possible removal of the alumina layer by the zinc chloride flux in the aluminum ATIG welding does not influence the weld bead geometry. It is observed that even for the thickness variations of the alumina layer taken into consideration, no significant variations were observed in the D/W ratio, remaining practically constant even with the weld bead volume changes.

3 Conclusions

From the results obtained in the simulations by varying the alumina layer on the TIG and ATIG welding process, there were no significant variations in the geometry of the weld bead. However, increasing the alumina layer, the depth of the bead decreased and the same occurred for the width.

The maximum temperature differences observed between TIG and ATIG aluminum welding are due to significant differences between the properties of the alumina layer and aluminum.

We considered a complete removal of the alumina layer from the specimen on the ATIG weld section. The simulation results showed that increasing the thickness of the alumina layer by 400% caused a reduction in the volume of the weld bead of only 14.22%. The results of the simulation performed in this study are similar to outcomes of previous works. Barroso et.al, for instance, showed that for aluminum or one of its alloys, the removal of the oxide layer obtained through the active flux application provides a superficial cleaning of the weld bead, but it does not work more effectively in obtaining a better Width / Depth ratio than in TIG welding.

Finally, we concluded that a possible removal of the alumina layer by the zinc chloride flux in the aluminum ATIG welding does not influence the weld bead geometry. It is noted that even for the thickness variations of the alumina layer considered, no significant variations were observed in the D/W ratio, remaining practically constant.

Acknowledgements. The authors would like to thank the Conselho Nacional de Desenvolvimento Científico Tecnológico (CNPq) for providing the Scientific Initiation Scholarship to the students motivated to carry out the experiments.

Authorship statement. The authors hereby confirm that they are the sole liable persons responsible for the authorship of this work, and that all material that has been herein included as part of the present paper is either the property (and authorship) of the authors, or has the permission of the owners to be included here.

References

[1] Schwartz, Mel. “Encyclopedia and handbook of materials, parts and finishes”. *CRC press*, 2016.
[2] Oliveira, W. C., 2007, “Study of the Effect of Fluxes on A-TIG Welding of Aluminum”, Ph.D. Thesis, School of Engineering/Universidade Federal de Minas Gerais, Belo Horizonte, 140 p., <http://hdl.handle.net/1843/MAPO-7RENCX>.

[3] Huang, Y., D. Fan, and F. Shao. "Alternative current flux zoned tungsten inert gas welding process for aluminium alloys." *Science and Technology of Welding and Joining* 17.2 (20)
[4] Vora, J. J.; Badheka, V. J. Experimental Investigation on Mechanism and Weld Morphology of "Activated TIG Welded Bead-on-plate Weldments of Reduced Activation Ferritic/ martensitic Steel Using Oxide Fluxes". J. *Manuf. Process*. Oct. 2015.
[5] Patel, Dixit; Jani, Suketu. "ATIG welding: a small step towards sustainable manufacturing." *Advances in Materials and Processing Technologies*, p. 1-23, 2020.
[6] M. Tanaka, T. Shimizu, T. Terasaki, M. Ushio, F. Koshiishi and C. L. Yang: Sci. Technol. Weld. Join., 2000, 6, 397–402.
[7] A. G. Simonik: *Weld. Prod*., 1976, 3, 49–51.
[8] C. R. Heiple and J. R. Roper: *Weld*. J., 1982, 61, 97–102.
[9] Zhang, R. H., and Ding Fan. "Numerical simulation of effects of activating flux on flow patterns and weld penetration in ATIG welding." *Science and Technology of welding and Joining* 12.1 (2007): 15-23.
[10] De Figueredo Barroso, Nelson, et al. "Effect of zncl2-Acetone Flux on ATIG Welding of Aluminum alloys. *8th Brazilian Congress of Manufacturing Engineering* (2015).
[11] Marques, Paulo Villani; Modenesi, Paulo José. "Algumas equações úteis em soldagem". *Soldag. insp*., São Paulo, v. 19, n. 1, p. 91-101, Mar. 2014.
[12] Garcez, Leonardo Riccioppo. *Investigação de métodos geradores de malhas aplicados a geometrias típicas das seções transversais de cabos umbilicais e tubos flexíveis*. 2017. PhD thesis. Universidade de São Paulo.
[13] Barros, Paternak de Souza. *Influência da convecção forçada em juntas soldadas*. MS thesis. Universidade Federal de Pernambuco, 2015.
[14] Cãngani, Ana Paula Mázaro. *Análise térmica do processo de soldagem TIG de amostras metálicas*. (2010).